Available online at www.sciencedirect.com
SCIENCE DIRECT
Journal of Chromatography A, 1102 (2006) 96–103
JOURNAL OF CHROMATOGRAPHY A
www.elsevier.com/locate/chroma

Ultra-rapid separation of an angiotensin mixture in nanochannels using shear-driven chromatography

Sarah Vankrunkelsven [a,*], David Clicq [a], Deirdre Cabooter [a], Wim De Malsche [a,b], J.G.E. Gardeniers [b], Gert Desmet [a]

[a] *Vrije Universiteit Brussel, Department of Chemical Engineering, Pleinlaan 2, 1050 Brussels, Belgium*
[b] *MESA+ Research Institute, University of Twente, P.O. Box 217, 7500 AE Enschede, The Netherlands*

Received 18 July 2005; received in revised form 10 October 2005; accepted 11 October 2005
Available online 27 October 2005

Abstract

The present paper reports on the separation of a mixture of fluorescein isothiocyanate-labeled angiotensin I and II peptides in a shear-driven nanochannel with a C_{18}-coating and using an eluent consisting of 5% acetonitrile in 0.02 M aqueous phosphate buffer at pH 6.5. The flat-rectangular nanochannel in fused silica consisted of an etched structure in combination with a flat moving wall. The very fast separation kinetics that can be achieved in a nanochannel allowed to separate the angiotensin peptides in less then 0.2 s in a distance of only 1.8 mm. Plate heights as small as 0.4 μm were calculated after substraction of the injection effect.

Keywords: Nanochannel; Angiotensins; Shear-driven chromatography; Peptides; Fluorescence; Band broadening

1. Introduction

Started out in the early 1990s [1–3], the field of miniaturized microfluidic devices has grown rapidly over the last years. Miniaturization of analytical chemical methods offer many advantages, including the reduced requirements for solvents and reagents, short reaction times, the possibility to build portable instruments, low cost, low power consumption, versatility in design, and possibility for parallel operation and integration with other miniaturized devices [4]. Miniaturization has lead to lab-on-a-chip devices where one or several separations are performed in microfluidic channels on a silicon or glass chip [5,6]. An example of these chip-based separations system is the combined nano high performance liquid chromatography (HPLC)/mass spectrometry (MS) polymer microfluidic chip that has recently been described and commercialized by researchers of the Agilent Laboratories [7]. The best liquid chromatography (LC) separation could be achieved when running the chip at flow rates between 200 and 300 nL/min. The column had a 75 μm × 50 μm cross-section and a length of 45 mm and the LC experiments took 40 min.

Although most systems have dimensions in the micrometer scale, more and more researchers start to look into the possibility to use sub-micron channels, entering the area of "nanofluidics" [8,9]. One of the motivations for this work is that reducing the system dimensions offers large advantages in liquid chromatography. Considering that the time needed to diffuse across a given distance d is according to Einstein's diffusion law roughly equal to $t = d^2/D_{mol}$, it follows immediately that performing an open-tubular LC (OT-LC) or capillary electrochromatography (CEC) separation in a channel that is only 0.1 μm deep instead of 10 μm would allow a 10 000-fold reduction of the separation time. Several methods for the fabrication of nanochannels with [10] or without nanoimprint lithography [11] have been investigated and pressure-driven as well as electrokinetic nanochannel flows have already been reported [12–16]. The nanochannel research also already focused on the selection of the most appropriate substrate materials, considering poly(dimethylsiloxane) (PDMS), silicon as well as glass substrates [17,18]. Eijkel et al. studied drying-out effects caused by osmosis and pervaporation through polyimide nanochannels [19]. Using optimized surface machining techniques also made it possible to produce channels with

* Corresponding author. Tel.: +32 2 629 37 81; fax: +32 2 629 32 48.
E-mail address: svkrunke@vub.ac.be (S. Vankrunkelsven).

0021-9673/$ – see front matter © 2006 Elsevier B.V. All rights reserved.
doi:10.1016/j.chroma.2005.10.017

lateral dimensions below 100 nm and to realize a pneumatically actuated, capillary-pressure-driven micropump capable of delivering picoliter amounts of liquid in a controlled way [20,21]. Nanochannels also have the advantages that their dimensions are smaller than the size of biological macromolecules, with potentially useful consequences for separations; they also have a very high ratio of surface to volume, and thus allow the study of wall effects in biological separations [22,23].

The two main methods for driving the flow of fluids in microchannels, pressure-driven and electrokinetic, however, each have their drawbacks. Pressure-driven flow performs poorly in assays requiring high-resolution separation because the velocity profile of a cross-section is parabolic, and samples in the form of plugs undergo axial dispersion and peak broadening. The main problem however is that extremely high inlet pressures are needed to drive the fluid flow through the narrow nanochannels. Electrokinetic flow also has important drawbacks for bioassays, including buffer incompatibility (only buffers of appropriate pH and ionic strength are compatible), the need for an off-chip power supply, electrolytic bubble formation, and evaporation of solvent due to heating [4]. The main problem with respect to nanochannel flow is that the electrical-double-layers that are formed at the channel walls start to overlap at the center of the channel. This leads to the formation of a more parabolic instead of a perfectly flat flow profile, and more importantly, also to a dramatic reduction of the achievable flow rate [24,25].

In the past few years, our group has been developing a shear-driven flow method that uses channels composed of two independent longitudinal walls kept together by applying a small normal load to the assembled system [26–30]. The fluid flow in this system is caused by the dragging effect originating from the movement of one channel wall while the other stays stationary (Fig. 1(a)). As described in [26], this leads to a linear velocity profile with a mean velocity equaling:

$$u = \frac{u_{\text{wall}}}{2} \tag{1}$$

The flow velocity is thus independent of the fluid viscosity and the channel depth and length, which allows the use of channels with very small depths at high fluid flow velocities [27]. Applying a retentive coating on the stationary wall then in principle allows to perform all forms of liquid chromatography without any restriction on the applicable fluid velocity or channel depth. In previous work, the practical feasibility of this shear-driven chromatography (SDC) principle has been demonstrated by separating a mixture of four coumarin dyes in sub-second times [31]. Whereas coumarin dyes are neutral compounds and have a high autofluorescence, the present study is devoted to demonstrate that the SDC principle can also be applied to separate ionisable species. The motivation for this work is that whereas HPLC and OT-LC are two-phase systems, the SDC channels have a third phase, i.e., the surface of the moving wall. This surface is as large as the stationary wall surface and hence makes up an important part of the channel. To have a minimal interference with the actual separation, this third phase (i.e., the moving wall) should be as inert as possible. Since uncoated glass substrates currently are the single cost-effective alternative to be used as the moving wall, the presence of the silanol groups on this surface can certainly be expected to compromise the inertness requirement in the case of ionisable components. It is therefore a priori not obvious that ionisable components can be separated with a high resolution.

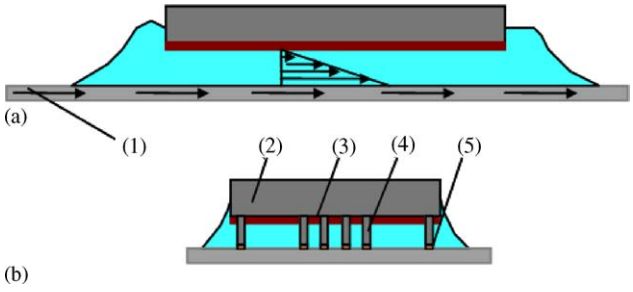

Fig. 1. Schematic cross-sectional (a) and longitudinal view (b) (not to scale) of the SDC operating principle, showing the dragging effect of the moving channel wall (1) and the resulting linear velocity profile. The etched fused silica platelet, the stationary channel wall, (size 10 mm × 20 mm) (2) put on top of this wafer, carried the C_{18} layer (3) and contained an array of parallel spacers (4). The lubrication layer (5) between the spacers and the moving wall is indicated as well.

As a model system, we selected the separation of two biologically important molecules: angiotensin I (ANG I) and angiotensin II (ANG II). The renin-angiotensin system is well known to be the most important pressor system in the body. In the circulatory system, angiotensins (ANGs), are potent vasoconstrictor peptides that play an important role in normal physiology processes and in various disease states [32]. Angiotensinogen is cleaved by the protease renin to produce ANG I, a biologically inactive decapeptide. The angiotensin converting enzyme removes the carboxyl terminal His-Leu from ANG I to produce the octapeptide ANG II, which explains the lower hydrophobicity of ANG II. ANG II is a potent pressor agent and the determination of angiotensins in mixtures is of interest in connection with the vital pressor mechanism.

2. Experimental

2.1. Chemicals

All chemicals were purchased at Sigma–Aldrich (Bornem, Belgium). ANG I and II were dissolved at a concentration of 4.3 mM in phosphate buffered saline (pH 7.4). Because of the required fluorescence detection, the samples were first labeled with fluorescein isothiocyanate (FITC) using the following protocol. First, a molar excess of FITC (dissolved in dimethylsulfoxide at a concentration of 0.05 M) was added to a mixture of 200 μl of the peptide solution and 20 μl of a 1 M sodium bicarbonate buffer (pH 9). The reaction was allowed to take place for 2 h at room temperature under constant stirring, protected from light. To remove the free dye, an extensive dialysis was performed using a dialysis membrane with a molecular weight cut-off (MWCO) of 500 (Float-a-Lyzer, Spectrum, Breda, The Netherlands) and a 0.02 M phosphate buffer (pH 6.5) as the dialysis buffer. Buffer volumes of 700 ml were replaced after 3 and

12 h and the dialysis continued overnight. In order to concentrate the diluted sample, the dialysis membrane was dried with Spectra/Por Gel Absorbent (Spectrum) until a final concentration of 2.9 and 2.1 mM for ANG I and II, respectively. The conjugate was subsequently divided into aliquots and stored at −20 °C.

At pH 6.50, the side chain contributions to the net charge of the ANG I and II peptides result in neutral molecules. However, labeling with FITC leads to an extra carboxyl group with a pK_a of 3 which results in a negatively charged molecule at pH 6.5.

2.2. Apparatus and experimental setup

The central part of the setup is the shear-driven flow channel, assembled by pressing two flat substrates (see Fig. 1) against each other: a small, rectangular fused silica platelet, with dimensions of 20 mm × 10 mm and carrying an array of parallel running channel spacers on its surface (see Figs. 1(b) and 2) and a larger, fully flat fused-silica wafer with a diameter of 5 cm, a thickness of 3 mm and with a flatness of λ/10 (Photox Optical Systems, Sheffield, UK). During the operation, the large fused-silica wafer is placed in a home-built metal holder that fits in the movable microscope table. The smaller stationary wall platelet is put on top of the fused-silica wafer and is kept stationary by fitting it into a home-built metallic holder. The channel spacers are used to maintain a fixed distance between both substrates. After assembly, the channels are positioned above the objective lens with 5× magnification (LMU-5×-266, OFR, Caldwell, UK) of an inverted fluorescence microscope (Axiovert 200, Zeiss, Zaventem, Belgium), using a system of in-house machined holding frames, as already described in [31,33]. In this way, the flow inside the SDC channels can be followed through the large transparent fused-silica wafer. The microscope is mounted on a breadboard (M-IG 23-2, Newport, Utrecht, The Netherlands), together with a linear displacement stage (M-TS100DC.5, Newport) equipped with a stepping motor (UE611CC, Newport) and a speed controller offering a total positioning accuracy of 0.5 μm (MM 4006, Newport). This displacement stage is used to automatically translate the microscope table, both during the injection procedure and during the subsequent flow experiments. The setup also contains a pneumatically operated metallic cover lid exerting a downward force on the upper (stationary) channel wall. This force is needed to keep the so-called lubrication layer, i.e., a thin layer of mobile-phase liquid that is always inevitably present between the channel spacers and the fused-silica plate (Fig. 1(b)), as thin as possible. Performing a series of flow control experiments with mobile-phase liquid containing 5 mM coumarin C_{440} dye, it was found [29] that a 1–2 bar pressure force was sufficient to keep the thickness of this lubrication layer below 10–20 nm, provided the channel substrate materials are sufficiently flat. A tight control of the lubrication layer thickness is needed to avoid too large run-to-run differences between the nominal channel depth determined via the WYKO scan and the effective channel depth that is experienced during the operation.

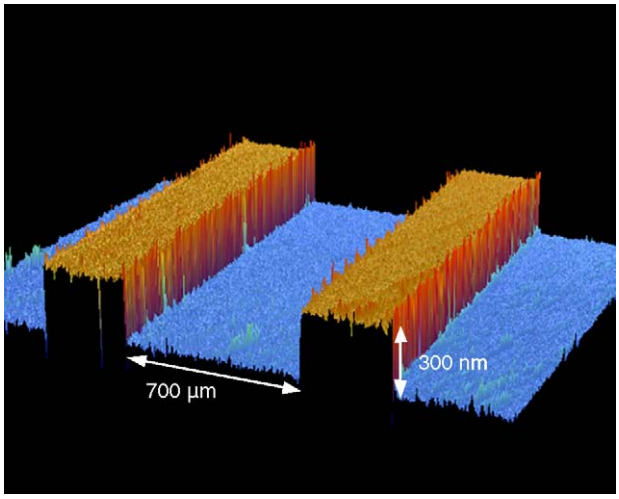

Fig. 2. WYKO®-surface scan measurement (IR interferometry) of a fused silica etched nanochannel of 300 nm used for SDC. The non-etched strips aside of the channel serve as spacers in the final channel assembly.

2.3. Channel manufacturing

The spacers shown in detail in Fig. 2 were obtained by etching the surface of round, fused silica wafers with a diameter of 4 in., a thickness of 2 mm and a flatness of λ/10 (Photox Optical Systems) via wet etching with HF. Inspection with a WYKO surface profilometer (Veeco Instruments, Cambridge, UK) revealed that the spacers had a nominal mean height of 300 nm. The etching mask was designed to yield three parallel running channels, each having a width of 700 μm and separated by 350 μm wide channel spacers. Prior to their use, an aluminium layer was sputtered on the backside of the fused silica platelets to reduce the background signal using a home built apparatus (Mesa + Institute, Enschede, The Netherlands). Subsequently, identical rectangles of 10 mm × 20 mm were diced (Disco DAD 321 Dicing Saw, Mesa + Institute) from the wafers, to yield the finally used stationary wall platelets.

2.4. Pretreatment and coating of the stationary wall platelets

The pretreatment of the stationary wall platelets was carried out according to a protocol described by Vidič et al. [34]. This consisted of first washing them with ethanol and deionized water to remove impurities, followed by boiling them for 3 h in deionized water. After this, the channels were rinsed with ethanol and dried overnight at 110 °C.

To apply a C_{18} stationary phase layer on the channels, the fused silica platelets were submersed in a 30% (v/v)-solution of chlorodimethyloctadecylsilane in toluene (Sigma–Aldrich, Bornem, Belgium) for 24 h at a temperature of 35 °C. The fused silica platelets were subsequently rinsed with toluene, acetone and methanol followed by drying them overnight at 110 °C, using the same procedure as described by Vidič et al. [34].

2.5. Contact angle measurement

The amount of bound silane was estimated qualitatively using contact angle measurements [34]. For this purpose, droplets of

10 μl deionized water were applied on the surface of the fused silica platelets and a picture was taken with a digital camera. The contact angle was subsequently determined by drawing a liquid surface tangent line at the contact point between the droplet and the solid surface, using National Instruments IMAQ Vision Builder 5.0 image analysis software to automatically read out the angle. Five measurements were taken for three different stationary wall platelets.

2.6. Injection, stopped-flow procedures

Sample plugs with a width of about 50 μm were injected in the channels using a multistep injection procedure already described in [35,36]. This procedure occurs in four successive steps. In the first step, the mobile phase present in front of the channel inlet is removed by aspirating it with a modified pipet tip connected to a vacuum pump (Pfeiffer, Asslar, Germany) via a thin plastic tube. In the second step, sample is loaded in front of the channel inlet using a standard micropipet. During the third step, the moving wall is displaced over a given prescribed distance (100 μm in the present case). This distance can be controlled to within 0.5 μm due to the displacement accuracy of the translation stage. This distance determines the width of the injected sample plug: neglecting diffusional contributions, the injected plug widths can be expected to be equal to the half of the displacement distance of the moving wall. During the fourth and final step, the displacement of the moving wall is briefly interrupted to aspirate the non-entered sample and to replace it by fresh mobile-phase liquid. When the injection sequence is fully completed, the actual flow experiment is started. To increase the resolution of the charge-coupled device (CCD)-camera image frames, the experiments were done in so-called stopped-flow conditions. For this purpose, the translation stage was programmed to stop abruptly after having traveled a known distance (3 mm in the present study). The displacement distance was selected such that it was sufficiently long to obtain a baseline separation of the peaks for all considered mobile phase velocities. In order to avoid additional diffusion band broadening, all analysis were performed on the first video frame captured after the displacement was halted. In all stopped-flow experiments, the frame illumination time was 0.04 s.

2.7. Detection

The FITC-labeling of the ANG samples allowed excitation by the blue light obtained by combining a mercury lamp (HBO 103/W2, Zeiss) and the blue filter cube set (11001v2, Chroma Technology, Rockingham, USA) of the microscope. The microscope images were recorded using an air-cooled CCD camera (ORCA-ER C4742-95, Hamamatsu Photonics, Louvain-la-Neuve, Belgium) mounted on the video adapter of the microscope. The camera was operated at a frame rate of 43 Hz in the 8×8 binning mode. The video frames were digitally captured using a Firewire interface. Subsequent analysis of the video images was carried out using the Simple-PCI 5.1 software accompanying the camera.

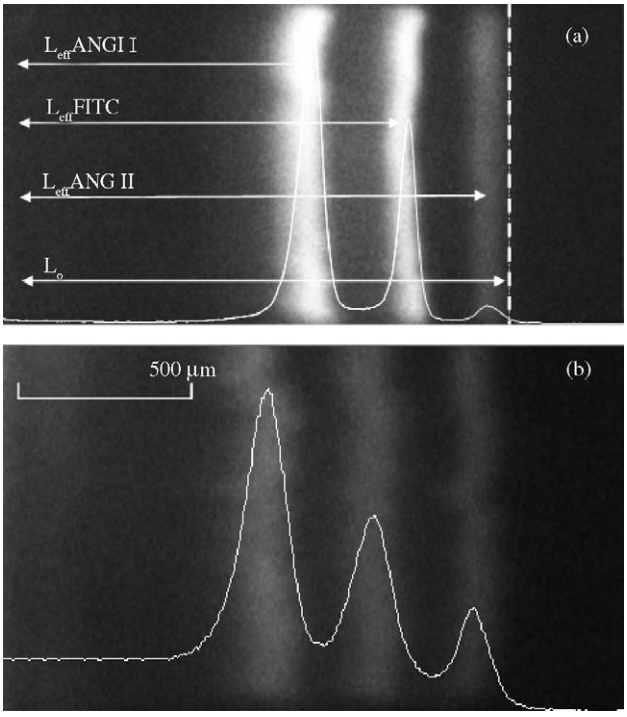

Fig. 3. Stopped-flow image taken with the CCD camera of a separation of the labeled angiotensin mixture at a moving wall velocity of (a) 2 mm/s and (b) 35 mm/s. Mobile phase: 5% (v/v) acetonitrile/0.02 M phosphate buffer pH 6.5.

2.8. Separation experiments

All separations were carried out at ambient temperature and under isocratic conditions in channels with a depth of 300 nm and a C_{18}-coating. Mobile phases containing 5–30% (v/v) acetonitrile in 0.02 M phosphate buffer at pH 6.50 were tested.

Using the still camera images, the retention factor k' of the sample components can be directly derived from the difference between the virtual position L_0 of the non-retained mobile phase liquid (moving with exactly one half of the moving wall velocity), and the actual position L_{eff} of the moving peak, using [35]:

$$k' = \frac{L_0 - L_{\text{eff}}}{L_{\text{eff}}} \tag{2}$$

The definition of L_0 and L_{eff} can also be assessed from Fig. 3.

Estimates of the plate height could be made from the variance ${\sigma_x}^2$ of the peaks. Assuming a Gaussian peak shape, a correction for the contribution of the initial width w of the injection plug was made according to:

$$H = \frac{\sigma_x^2 - \sigma_{x\text{inj}}^2}{L_{\text{eff}}} \quad \text{where} \quad \sigma_{x\text{inj}}^2 = \frac{w^2}{16} \tag{3}$$

3. Results and discussion

3.1. Coating experiments

The following three cases were studied in the contact angle measurements: non-coated channels, C_{18} coated channels without and with the pretreatment. These experiments clearly showed

the higher hydrophobicity of the coated channels compared to the untreated ones. The results were $20 \pm 1^\circ$, $36 \pm 1^\circ$ and $78 \pm 2^\circ$, respectively. The amount of bound silane was hence significantly larger when the substrates were subjected to the pretreatment. All channels used further in the study were therefore coated using the pretreatment method developed by Vidič et al. [34].

3.2. Separation experiments with variable mobile phase composition

In a first series of experiments, the amount of acetonitrile in the mobile phase of the separation experiments was varied from 5 to 30% (v/v) while the moving wall velocity was kept constant at 2 mm/s.

Fig. 3(a) shows a typical separation example obtained with 5% acetonitrile in the mobile phase. An overlay plot of the pixel intensity values, generated with the software program Simple PCI 5.1 is also shown in the image. This overlay plot clearly shows that the three peaks are baseline separated in distance of less than 2 mm. The peaks are not completely straight due to small channel inlet defects caused by the sawing of the fused silica wafer.

A first finding concerned the number of peaks: injections of the ANG mixture lead to three peaks instead of the expected two. Although extensive dialysis was performed after the labeling of the peptides, this could have been insufficient to remove all the free label used the labeling reaction. Injections of a pure FITC sample showed that this third peak could indeed be identified as the signal of the free FITC label. Removing the fluorescent label completely seems to be impossible with the available dialysis membranes: a membrane with a MWCO of 500 had to be used to remove the FITC molecules with a molecular weight of 389. Membranes with a higher MWCO would have failed to retain the ANG peptides.

For each injection, the distances traveled by the three peaks (unbound FITC-label and the labeled ANG I and II) were calculated as indicated in Fig. 3. The virtual position L_0 of the non-retained mobile phase liquid (moving with exactly one half of the moving wall velocity) is also indicated. The retention factors k' were subsequently calculated using Eq. (2). Fig. 4 shows a plot of the retention factor k' of the ANG and FITC mixture as a function of the percentage acetonitrile in the mobile phase. An acetonitrile concentration of 5 and 10% (v/v) resulted in separation of the three components. The separation was not complete at a concentration of 15% acetonitrile. A further increase of the acetonitrile amount lead to a co-elution of the components as a single band.

The mobile phase consisting of 5% acetonitrile in 0.02 M phosphate buffer, pH 6.50 (v/v) yielded optimal separations and was used in the remainder of the study. At 2 mm/s the retention factor equaled 0.40 (standard deviation = 0.05) for the ANG I, 0.12 (standard deviation = 0.03) for FITC and 0.01 (standard deviation = 0.03) for ANG II. These values show that the least hydrophobic peptide, ANG II, is almost not retained by the stationary phase.

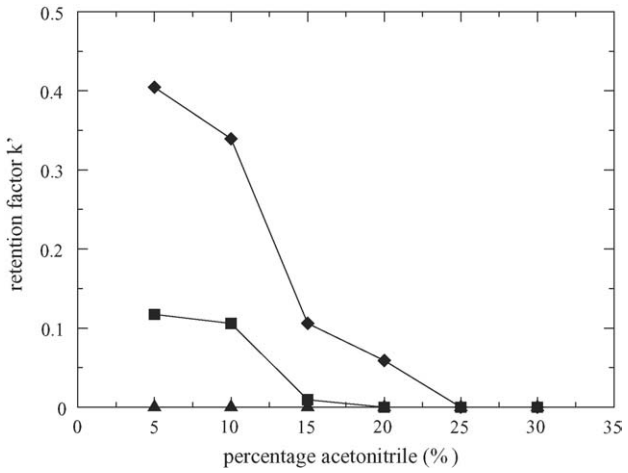

Fig. 4. Plot of the retention factor k' of the ANG and FITC mixture as a function of the percentage acetonitrile in the mobile phase. The moving wall velocity was 2 mm/s.

This is also reflected in the low amount of organic modifier in the mobile phase we need to use compared to other systems. Acetonitrile concentrations of 20% (v/v) and gradients ranging from 15 to 70% acetonitrile have been found in literature [37–39]. The retention strength of the applied monolayer coating is hence clearly lower than in packed bed columns. Comparing the surface to volume ratios of the open-tubular rectangular SDC channels and the packed bed columns explains this. The employed SDC channels indeed have a surface to volume ratio of $1/d$, with d the channel depth, which results in a 100 times lower value than for a typical packed bed. The monolayer coating applied on the SDC channels hence has a 100 times less retention capacity. A possible solution to improve this would be the creation of a thin layer (100–200 nm thick) of porous silicon stationary phase [33].

3.3. Separation experiments with variable velocity

Subsequently a series of separation experiments was conducted at different moving wall velocities, ranging from 1 to 35 mm/s. In all these experiments the mobile phase had a composition of 5% (v/v) acetonitrile in 0.02 M phosphate buffer (pH 6.5).

As shown in Fig. 3(b), the mixture can still be separated in the first 2 mm of the channel at the largest moving wall velocity of (i.e., 35 mm/s) that can be achieved with the currently employed translation stage. At this velocity, the ANG mixture is separated in just 0.17 s. This is a dramatic gain compared with the separation time of about 20 min needed in [37] for a conventional reversed phase packed-bed HPLC separation of a mixture of ANG I and II, and working also in isocratic conditions at pH 6.5, with a mobile phase containing 20% (v/v) acetonitrile in a 10 mM phosphate buffer. The reason for the much faster separation in the SDC system obviously is due to the much smaller mass transfer distances between the mobile and the stationary phase which leads to a faster separation of the components in a mixture [40].

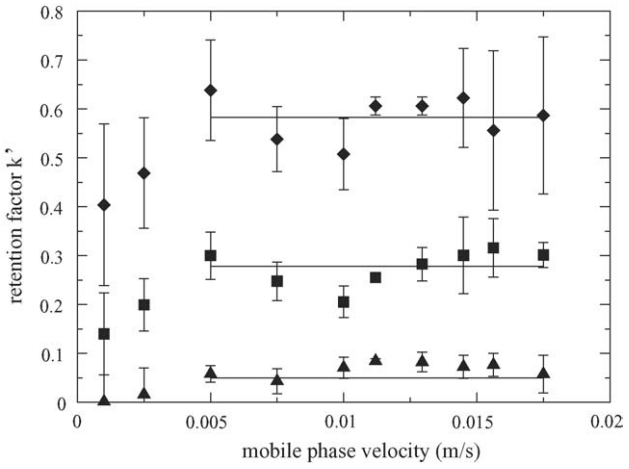

Fig. 5. Retention factors of ANG I (♦), FITC (■) and ANG II (▲) as a function of the mobile phase velocity. The shown values are the average of three experimental measurements with their standard deviation.

Fig. 5 shows the observed retention factors k' as a function of the mobile phase velocity. The error bars indicate quite large run-to-run differences. At present, we assume that these originate from the difficulty to precisely control the thickness of the lubrication layer probably caused by imperfections on the employed metallic holder systems. Another important observation that needs to be made is that the retention was significantly smaller for the two smallest velocities (1 and 2.5 mm/s) than for the other, higher velocities. A similar observation was made in previous work [29] but up to now no explanation for this phenomenon could be formulated for this, especially because a reduced retention would be more expected to occur at the higher end of the velocity range. At higher velocities the adsorption process could be expected to occur less efficiently which would lead to lower retention factors.

Experimentally obtained plate heights were calculated from the measurements of the peak variances (Fig. 3) using Eq. (3). Instead of using the entire width of the channel, only a slice of about 100 μm of the peak is used for the calculations. The value of the variance that was substracted out for the injection peak was found to be 2.8×10^{-10} m^2. These values were compared with theoretical values for the plate heights which could be calculated using the following expression for a shear-driven flow through an open tubular channel with a flat-rectangular cross-section [26]:

$$H = 2\frac{D_m}{u} + \frac{2}{30}\frac{1+7k+16k^2}{(1+k)^2}u\frac{d^2}{D_m} + \frac{2}{3}\frac{k}{(1+k)^2}u\frac{d_f^2}{D_s} \quad (4)$$

using molecular diffusion constant values of 1.9×10^{-10}, 5.4×10^{-10} and 2.3×10^{-10} m^2/s for ANG I, FITC and ANG II, respectively. These diffusion constants were measured experimentally using a shear-driven technique described in [41]. Given that only a monolayer coating was applied, d_f is negligibly small and the last term of Eq. (4) can hence be cancelled.

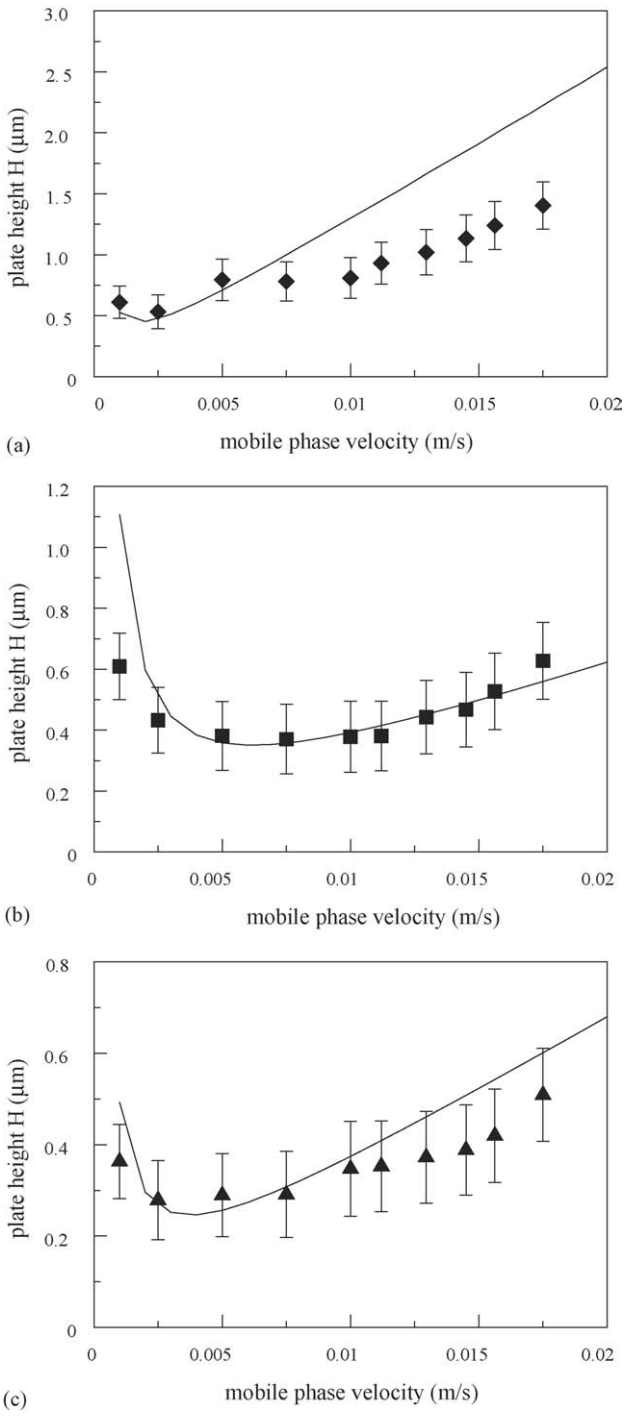

Fig. 6. Experimental plate heights (points) as a function of the mobile phase velocity obtained during a series of angiotensin separations in a C_{18} coated channel with a depth of 300 nm. Mobile phase: 5% (v/v) acetonitrile/0.02 M phosphate buffer at pH 6.5. The theoretical values (full lines) are obtained by putting in Eq. (4) $d = 300$ nm, $d_f = 0$ and $D_m = 1.9 \times 10^{-10}$, 5.4×10^{-10} and 2.3×10^{-10} m^2/s for ANG I (a), FITC (b) and ANG II (c), respectively.

Fig. 6(a)–(c) show the plate heights in function of the mobile phase velocity of the components ANG I (a), FITC (b) and ANG II (c). Every measurement is the average of three experiments, the error bars were calculated with Eq. (5), obtained by applying the error propagation rules to Eq. (3) and showing that the error on the measurements (ΔH) was composed of the following three

terms:

$$\Delta H = \left| -\frac{1}{16}\frac{W_{b,x=L}^2 - W_{b,x=0}^2}{L^2}\Delta L \right| + \left| \frac{W_{b,x=L}}{8L}\Delta W_{b,x=L} \right| + \left| \frac{W_{b,x=0}}{8L}\Delta W_{b,x=0} \right| \quad (5)$$

where the first term represents the error on the distance L that is measured and the other terms the error on the peak widths at $x = L$ and $x = 0$, respectively. In Eq. (5) $\Delta W_{b,x=L}$ is the width of the peak at the basis at position $x = L$ (m), $\Delta W_{b,x=0}$ the width of the peak at the basis at position $x = 0$ (m), L the traveled distance of the band (m). ΔL is the error on L (m), while $\Delta W_{b,x=L}$ and $\Delta W_{b,x=0}$ are the errors on the peak width at the basis at position $x = L$ (m) and at position $x = 0$ (m), respectively. The value for ΔL, $\Delta W_{b,x=L}$ and $\Delta W_{b,x=0}$ was taken to be equal to 6 μm, corresponding to the width of a single pixel.

Fig. 6(a)–(c) show that the optimal mobile phase velocity for the separation of the mixture in a 300 nm deep channel is about 3 mm/s. The plate height at this velocity is only 0.4 μm, i.e., about 20 times smaller than in packed bed HPLC where typical plate heights are 6–10 μm [42].

4. Conclusion

Shear-driven chromatography allowed to separate a mixture of ANG peptides in a very short time (less than 0.2 s) in a distance of only 2 mm. Plate heights are over an order of magnitude smaller than can be achieved in traditional HPLC systems. The good separation properties are due to the fact that the neutralization of the angiotensins at pH 6.5 reduced the (undesired) interactions with the silanol groups on the moving glass wall.

A further improvement would be possible if channels with a smaller depth in the order of 100 nm or less, could be used. Unfortunately, detection then becomes more and more difficult because the number of detectable molecules is reduced. To improve the detection, switching from a lamp to a monochromate laser as the excitement source, and switching to a photomultiplier tube as the detector instead of using a CCD camera, would already constitute a large advantage. Also the application of thin porous layers that are more retentive than the currently employed C18 monolayer are needed.

Acknowledgements

The authors gratefully acknowledge financial support from the Fonds voor Wetenschappelijk Onderzoek (FWO, grant no. G.0042.03) and the Instituut voor Wetenschap en Technologie (IWT, grant no. GBOU/010052). D.C. is a post-doc research fellow of the Fonds voor Wetenschappelijk Onderzoek (FWO).

References

[1] A. Manz, N. Graber, H.M. Widmer, Sens. Actuators B 1 (1990) 244.
[2] A. Manz, Y. Miyhara, J. Miura, Y. Watanabe, H. Miyagi, K. Sato, Sens. Actuators B 1 (1990) 249.
[3] D.J. Harrison, A. Manz, Z.H. Fan, H. Ludi, H.M. Widmer, Anal. Chem. 64 (1992) 1926.
[4] S.K. Sia, G.M. Whitesides, Electrophoresis 24 (2003) 3563.
[5] M. Szumski, B. Buszewski, Crit. Rev. Anal. Chem. 32 (2002) 1.
[6] J.G.E. Gardeniers, A. van den Berg, Anal. Bioanal. Chem. 378 (2004) 1700.
[7] H. Yin, K. Killeen, R. Brennen, D. Sobek, M. Werlich, T. van de Goor, Anal. Chem. 77 (2005) 527.
[8] T. Tsukahara, A. Hibara, T. Kitamori, in: T. Laurell, J. Nilsson, K. Jensen, D.J. Harrison, J.P. Kutter (Eds.), Proceedings of Micro Total Analysis Systems 2004, vol. 2, Athenaeum Press, Gateshead, UK, 2004, p. 189.
[9] M. Foquet, J. Korlach, W.R. Zipfel, W.W. Webb, H.G. Craighead, Anal. Chem. 76 (2004) 1618.
[10] X. Cheng, L.J. Guo, C. Chou, in: M.A. Northrup, K.F. Jensen, D.J. Harrison (Eds.), Proceedings of Micro Total Analysis Systems 2003, Mesa Monographs, vol. 1, 2003, p. 709.
[11] C. Lee, E. Yang, N.V. Myung, T. George, in: M.A. Northrup, K.F. Jensen, D.J. Harrison (Eds.), Proceedings of Micro Total Analysis Systems 2003. Mesa Monographs, vol. 1, 2003, p. 643.
[12] S.C. Jacobson, J.P. Alarie, J.M. Ramsey, in: J.M. Ramsey, A. van den Berg (Eds.), Proceedings of Micro Total Analysis Systems 2001, Kluwer Academic Publishers, Norwell, MA, 2001, p. 57.
[13] J.P. Alarie, A.B. Hmelo, S.C. Jacobson, A.P. Baddorf, L. Feldman, J.M. Ramsey, in: M.A. Northrup, K.F. Jensen, D.J. Harrison (Eds.), Proceedings of Micro Total Analysis Systems 2003, Mesa Monographs, vol. 1, 2003, p. 9.
[14] N.J. Petersen, J.P. Alarie, S.C. Jacobson, J.M. Ramsey, in: M.A. Northrup, K.F. Jensen, D.J. Harrison (Eds.), Proceedings of Micro Total Analysis Systems 2003, Mesa Monographs, vol. 1, 2003, p. 701.
[15] S. Pennathur, J.G. Santiago, in: T. Laurell, J. Nilsson, K. Jensen, D.J. Harrison, J.P. Kutter (Eds.), Proceedings of Micro Total Analysis Systems 2004, vol. 1, Athenaeum Press, Gateshead, UK, 2004, p. 402.
[16] E. Tamaki, A. Hibara, H. Kim, M. Tokeshi, T. Ooi, M. Nakao, T. Kitamori, in: T. Laurell, J. Nilsson, K. Jensen, D.J. Harrison, J.P. Kutter (Eds.), Proceedings of Micro Total Analysis Systems 2004, vol. 1, Athenaeum Press, Gateshead, UK, 2004, p. 318.
[17] V.G. Kutchoukov, F. Laugere, W. Van der Vlist, L. Pakula, Y. Garini, A. Bossche, Sens. Actuators A 114 (2004) 521.
[18] T.S. Hug, D. Parrat, P.-A. Künzi, U. Staufer, E. Verpoorte, N.F. De Rooij, in: M.A. Northrup, K.F. Jensen, D.J. Harrison (Eds.), Proceedings of Micro Total Analysis Systems 2003, Mesa Monographs, vol. 1, 2003, p. 29.
[19] J.C.T. Eijkel, J.G. Bomer, A. van den Berg, in: T. Laurell, J. Nilsson, K. Jensen, D.J. Harrison, J.P. Kutter (Eds.), Proceedings of Micro Total Analysis Systems 2004, vol. 1, Athenaeum Press, Gateshead, UK, 2004, p. 405.
[20] N.R. Tas, J.W. Berenschot, P. Mela, H.V. Hansen, M. Elwenspoek, A. van den Berg, Nano Lett. 2 (2002) 1031.
[21] N.R. Tas, J.W. Berenschot, T.S.J. Lammerink, M. Elwenspoek, A. van den Berg, Anal. Chem. 74 (2002) 2224.
[22] G.M. Whitesides, Nat. Biotechnol. 21 (2003) 1161.
[23] S. Vankrunkelsven, D. Clicq, K. Pappaert, G.V. Baron, G. Desmet, Anal. Chem. 76 (2004) 3005.
[24] C.L. Rice, R. Whitehead, J. Phys. Chem. 69 (1965) 4017.
[25] R. Stol, Capillary Electrochromatography with Porous Particles, Universal Press, Amsterdam, The Netherlands, 2002, p. 217.
[26] G. Desmet, G.V. Baron, J. Chromatogr. A 855 (1999) 57.
[27] G. Desmet, G.V. Baron, Anal. Chem. 72 (2000) 2160.
[28] D. Clicq, N. Vervoort, R. Vounckx, H. Ottevaere, J. Buijs, C. Gooijer, F. Ariese, G.V. Baron, G. Desmet, J. Chromatogr. A 979 (2002) 33.
[29] D. Clicq, S. Vankrunkelsven, W. Ranson, C. De Tandt, G.V. Baron, G. Desmet, Anal. Chim. Acta 507 (2004) 79.
[30] D. Clicq, N. Vervoort, W. Ranson, C. De Tandt, H. Ottevaere, G.V. Baron, G. Desmet, Chem. Eng. Sci. 59 (2004) 2783.
[31] D. Clicq, N. Vervoort, G.V. Baron, G. Desmet, LC–GC Eur. 17 (2004) 278.

[32] S. Oparil, E. Haber, N. Engl. J. Med. 291 (1974), pp. 389, 446.
[33] D. Clicq, R.W. Tjerkstra, J.G.E. Gardeniers, A. van den Berg, G.V. Baron, G. Desmet, J. Chromatogr. A 1032 (2004) 185.
[34] J. Vidič, A. Podgornik, A. Štrancar, J. Chromatogr. A 1065 (2005) 51.
[35] G. Desmet, N. Vervoort, D. Clicq, G.V. Baron, J. Chromatogr. A 924 (2001) 111.
[36] G. Desmet, N. Vervoort, D. Clicq, A. Huau, P. Gzil, G.V. Baron, J. Chromatogr. A 948 (2002) 19.
[37] Q.C. Meng, J. Durand, Y.-F. Chen, S. Oparil, J. Chromatogr. 614 (1993) 19.
[38] D. Carr (Ed.), The Handbook of Analysis and Purification of Peptides and Proteins by Reversed-Phase HPLC, Advanstar, New York, United States, 2002, p. 69.
[39] J. Mohammad, B. Jäderlund, H. Lindblom, J. Chromatogr. A 852 (1999) 255.
[40] S.C. Jacobson, R. Hergenröder, L.B. Koutny, J.M. Ramsey, Anal. Chem. 66 (1994) 1114.
[41] K. Pappaert, J. Biesemans, D. Clicq, S. Vankrunkelsven, G. Desmet, Lab Chip 5 (2005) 1104.
[42] C.F. Poole, S.K. Poole, Chromatography Today, Elsevier Science Publishers, Amsterdam, The Netherlands, 1991, p. 1027.